Polymer Trace Devolatilization: I. Foaming Experiments and Model Development

Chi-Tai Yang and Theodore G. Smith
Dept. of Chemical Engineering, University of Maryland, College Park, MD 20742

David I. Bigio
Dept. of Mechanical Engineering, University of Maryland, College Park, MD 20742

Colin Anolick
Central Research and Development Dept., DuPont, Wilmington, DE 19880

Volatile species are removed from polymers by devolatilization. Foaming experiments using corn syrup and low-density polyethylene were carried out to investigate effects of volatile content, operating vacuum level and stripping agent in devolatilization. When foaming and rupture occur, a limiting foam volume growth was observed for a polymer regardless of the volatile content and the addition of stripper bubbles. A mathematical model was also developed to study the effect of stripper bubbles in polymer devolatilization. Based on the cell model for bubble growth, a bimodal model for foam growth is developed as the first step to describe the initial formation and growth of the volatile and stripper bubbles in polymer during devolatilization. When foaming and breakup occur at a critical foam volume expansion, a film model for mass transfer is used to model the second step of devolatilization. A numerical factorial study shows that the devolatilization section should be designed and operated to provide the screw channel sufficient free volume and residence time for the desired foam expansion.

Introduction

Removal of residual volatile components from polymer melts or solutions during the manufacturing process has been a very important operation in polymer processing. These residual low-molecular-weight species can be unreacted monomers, reaction byproducts, solvents, or impurities. Their removal is needed in condensation polymerization to obtain high molecular weight polymers. Low volatile levels are also needed for the safe shipment of the polymers, and the emission regulations set by EPA or OSHA. In industrial practice, the removal of residual volatile components is often achieved by a process called "devolatilization." This process involves the application of a reduced pressure or vacuum to extract volatile vapors, and often the injection of a stripping agent to enhance devolatilization efficiency. As a result, the devolatilization process often generates bubbles of the volatile components and the stripping agents. Stripping agents are often inert media; steam (water) and nitrogen are two commonly used stripping agents (Biesenberger and Sebastian, 1983). The various aspects of polymer devolatilization have been reviewed in the literature (Werner, 1980; Biesenberger and Sebastian, 1983; Biesenberger, 1983; Denson, 1983; Albalak, 1996).

Several types of mass-transfer equipment are used to handle the polymer during the devolatilization process including extruders, wiped film evaporators, flash separators, and drum dryers. In this work, we focus on polymer devolatilization in screw extruders, but many of the remarks and theories apply to other equipment types as well.

Correspondence concerning this article should be addressed to D. I. Bigio.
Current address of C.-T. Yang: Formosa Plastics Corporation, P.O. Box 320, Delaware City, DE 19706.

There have been two major types of models describing the devolatilization process in the literature: the "pool model" and the "foam model." The pool model uses the classical penetration theory for mass transfer to describe devolatilization. It assumes that volatile components are removed from the polymer by diffusion of the dissolved volatile component from the polymer phase, through the polymer-gas interface and into the contiguous gas phase (Latinen, 1962; Coughlin and Canevari, 1969; Roberts, 1970; Biesenberger and Kessidis, 1982; Collins et al., 1985; Secor, 1986). The diffusion process of the volatile component in the polymer pool through foam generation is not considered in this model. In extruder processes, screw rotation results in surface renewal and enhances the mass transfer in devolatilization. Therefore, by this model, the capabilities of the extruders to continuously generate free surface area is very important. The pool model predicts that the mass-transfer process is limited by the low diffusion coefficient of the volatile component in the polymer. In general, pool models fail since the actual mass-transfer rates obtained by experiments greatly exceed those calculated by the penetration diffusion theory.

The foam model assumes that volatile components are removed from the polymer by a sequence of complicated bubble transport mechanisms in devolatilization. These mechanisms include bubble nucleation (Foster and Lindt, 1990), bubble growth (Newman and Simon, 1980; Yoo and Han, 1984; Denson, 1983; Amon and Denson, 1984; Powell, 1987; Foster and Lindt, 1989, 1990), bubble motion, coalescence and rupture (Foster and Lindt, 1990) and removal under vacuum. In industrial practice, bubbles can be generated from exposing polymer solutions to a reduced pressure or even a vacuum and/or injecting a stripping agent into the polymer. The bubble generation creates more internal surface area and shortens the diffusion path for the mass transfer of the volatile components in the polymer. Foam devolatilization is a much faster mass-transfer process compared to devolatilization by molecular diffusion.

In the foam model, the bubble nucleation is assumed to occur instantaneously with a given initial number of bubbles. The bubble growth is often described by two types of bubble dynamic theories. One theory is the single bubble growth model, the other theory is the cell model for bubble growth. These theories are based on the bubble growth in a static model. The single bubble growth model assumes a single spherical bubble growing in a quiescent infinite sea of liquid medium (Newman and Simon, 1980; Yoo and Han, 1984). The cell model assumes many spherical bubbles growing together with a thin shell of liquid film surrounding them (Denson, 1983; Amon and Denson, 1984; Powell, 1987; Foster and Lindt, 1990). The cell model is more realistic since it considers the effects of adjacent bubbles in mass transfer. The bubble motion and coalescence are not well described and only the research done by Foster and Lindt gave a criterion for bubble rupture. It is important to note that the separation of the volatile components from the liquid phase into the growing bubbles is only part of the devolatilization process. Devolatilization is only complete when the volatile component is transferred to a foam free surface or the bubbles rupture giving a free path for the volatiles to separate. More research needs to be done in the area of bubble coalescence and rupture to make the foam model more complete. In addition, a way to predict the initial number of bubbles is needed.

In addition to theoretical modeling, experimental work has been done to observe the foam formation and growth in polymer devolatilization. Biesenberger and Lee (1986a,b; 1987a,b; 1989) conducted a series of experiments on foam-enhanced polymer devolatilization in a special apparatus, which combines a blade and a rotating glass drum in order to simulate the flow configuration in industrial rotary devolatilization machines. They observed that the intensity of foam activity increased with the degree of supersaturation and rotational speed beyond the threshold level (on the order of 100 mm Hg or more). Albalak et al. (1987, 1990) examined polymer melt devolatilization mechanism in a falling-strand devolatilizer. Polymer melt was fed into a preheated chamber operated at the desired vacuum pressure. Polymer melt samples were collected at different times. The samples were quenched under liquid nitrogen for morphological studies by scanning electron microscopy (SEM). Their observations from SEM showed that the falling-strand devolatilization was accomplished through a series of complex bubble transport phenomena. Swarms of randomly distributed large voids were observed in the core and on the lateral surface of the melt strand. These macrobubbles are on the order of 100 μm. The inner surface of a macrobubbles was found to have some blisters (about 1 to 100 μm in diameter) which grew, burst, and renucleated repeatedly. Tukachinsky et al. (1993) applied ultrasound to the polymer melt extruded into a vacuum chamber. They found that the equilibrium gaseous nuclei within the polymer melt were activated into bubble growth centers when the polymer melt is superheated. The acoustic field causes high-frequency stretch-compression stresses within the polymer melt creating areas of tiny bubbles (acoustic cavitation). As a result, the acoustic treatment helps the polymer melt to foam up visibly, even at atmospheric pressure conditions, and improve the devolatilization efficiency. In a later study, Tukachinsky et al. (1994) used the SEM technique reported by Albalak et al. (1987, 1990) to investigate foam-enhanced devolatilization of polystyrene melt in a 50 mm vented single-screw extruder. Similar bubble dynamics in bubble formation, growth and burst was observed. Vigorous foaming was found to begin earlier and ends sooner than during falling-strand devolatilization under similar conditions. The shear force elongates the macrobubbles and develops stretching stresses on the polymer surface near the shell of a growing blister. Such stretching stress can facilitate bubble nucleation. Under steady-state conditions, foaming of the polymer melt takes place only in the starting section of the screw in no more than two leads of its length and foaming is completed within three screw turns.

Even through the injection of stripping agents has long been an industrial practice to enhance the devolatilization performance in an extruder, very few articles have been published in examining the roles of stripping agents. It is generally accepted that this inert gas component functions by reducing the partial vapor pressure of the dissolved volatile component in the gas phase, thus increasing the thermodynamic driving force for mass transfer. The stripping agent can assist in creating more free surface area for mass transfer by generating bubbles. Vrentas et al. (1985) analyzed the desorption of a volatile component from a stagnant polymer film

by sweeping an inert gas stream (stripping agent) through the polymer interface. Ravindranath and Mashelkar (1988) modeled the role of dissolved stripping agents in polymer devolatilization. These studies focused on the effect of a third inert component (stripping agent) on devolatilization of a volatile component present in a stagnant polymer film. The presence of dissolved stripping agents in the polymer was found to increase the free volume of the polymer, which increases the apparent diffusion coefficient of the volatile component. By applying the free-volume theory in the prediction of diffusion coefficients in polymer-solvent systems (Vrentas and Duda, 1976, 1977a,b; Zielinski and Duda, 1992), it has been shown that 1.0 wt. % of dissolved nitrogen (stripping agent) can enhance the apparent diffusion coefficient of ethylbenzene (volatile component) in polystyrene at 150°C by 9% (Yang, 1995; Yang et al., 1996a). However, considering the low diffusion coefficients of stripping agents in the polymer (on the order of 10^{-6} to 10^{-5} cm^2/s), it may take several hours for stripping agents to dissolve in the polymer. Since the average residence time of a stripping agent in an extruder is very short, typically about 5 to 10 s, there is not sufficient time for a stripping agent to dissolve in the polymer liquid phase. Consequently, a predominant fraction of the stripping agent should stay in the gas phase either dispersing in the polymer as bubbles or sweeping over the polymer surface.

Werner (1980) reported that the addition of a stripping agent can make the polymer melt foam so that the bubbles provide an additional exposed melt surface for devolatilization. In order to achieve this, the stripping agent must be thoroughly mixed to the polymer under pressure. The mechanism for mixing of the stripping agent in the polymer was not described. Mack and Pfeiffer (1993) applied a fiber optic method to investigate the mixing quality of water as a stripping agent in polymer devolatilization. They found that the fiber optic technique cannot quantify the drop sizes. In a recent article, Barth et al. (1995) reported devolatilization in a multiscrew extruder using water and nitrogen as the stripping agents. Under a high melt pressure, the mixing section in the extruder can incorporate the stripping agent and create foaming. The screw configuration was not revealed which could have permitted a better understanding toward the devolatilization dynamics enhanced by the bubbles of the stripping agents.

The objectives of this research have been to examine the devolatilization role of stripping agents in devolatilization performance and investigate the rate of approach to thermodynamic equilibrium in polymer devolatilization. First, we report the results of batch foaming experiments using both a model fluid (corn syrup) at room temperature and a synthetic polymer (low density polyethylene) at higher temperature. Based on the observation of the foaming experiments and the cell model for devolatilization, a mathematical model is developed to investigate the effect of stripper bubbles on foam dynamics and devolatilization performance (Yang et al., 1996a,b). Comparison of our model with the cell model and experimental verification of our model are presented in Yang et al. (1997).

Foaming Experiments

Materials

Corn syrup was used as a model fluid in this research. Its specific gravity is 1.4 g/cm^3 and its viscosity is reported nominally as 56 Pa·s. Carbon dioxide (Cole Palmer grade, supplied by Air Products and Chemical, Inc.) was used as a volatile gas in corn syrup. The synthetic polymer used in the foaming experiment is low density polyethylene (LDPE, tradename Sclair) manufactured by DuPont Canada. The specific gravity of LDPE is 0.92, and the typical crystallinity index is about 50%. Nitrogen was used as the stripping agent in both foaming experiments.

Model Fluid-Corn Syrup

An independent experiment was performed to determine the solubility of carbon dioxide in the corn syrup used. The solubility value was reported as 0.333 cm^3 at STP/g·atm at 25°C (Yang, 1995).

The experimental setup used in the corn syrup foaming experiments is shown in Figure 1. The test chamber is a modified version of a slit rheometer, which is composed of three pieces of Invar-36 slit die element. The top element was replaced with a clear polycarbonate plate for visualization. An aluminum plate with a pinhole at the center was fitted into the position where the rectangular transverse slot was originally located. A gas manifold connected with four U-tube glass traps was used to condense volatile vapors under liquid nitrogen at different time intervals.

Effects of Volatile Content and Vacuum Pressure. For the first set of batch devolatilization experiments, the initial carbon dioxide concentration in corn syrup was varied at the solubility values at 60 and 30 psig (515 and 308 kPa). They correspond to the initial concentration 0.14 wt. % and 0.085 wt. %, respectively. The corn syrup, contained with carbon dioxide, was then pumped into the test chamber until its height reached about 1 cm. Different levels of vacuum [380, 200, 125, 75, 50 and 25 mmHg (51, 27, 17, 10, 7 and 3 kPa)] was applied to the test chamber to start the foaming process. The foaming process was videotaped and foam height developed in the experiments was recorded. To determine the effect of the stripping agent on devolatilization, 0.1 wt. % nitrogen was injected to the test chamber as the stripping agent for the same conditions in the second set of experiments. After devolatilization, carbon dioxide was collected at four time intervals (0–1, 1–3, 3–5 and 5–10 min). The traps were brought up to room temperature after experiments to determine the vapor pressure of carbon dioxide.

Figure 2 shows the foam volume change with time at 0.14 wt. % initial carbon dioxide concentration [60 psig (515 kPa) initial carbon dioxide pressure] under different vacuum conditions. Experimental results from the 60 psig (515 kPa) initial carbon dioxide pressure and 25 mm Hg (3 kPa) vacuum condition showed that corn syrup foamed up very quickly within 15 s. The foam rose up substantially and bubbles grew bigger via volume expansion, mass diffusion and coalescence with neighboring bubbles. Vigorous foam activity was observed such as boiling. Some foam rupture was also observed near the free foam surface. Finally, the foam reached about five times the initial volume. The foam had a cellular structure with thin liquid films distributed in between the larger bubbles. The shape of the foam cells were not spherical. The larger bubbles, especially the ones closer to the foam surface, were elongated into a tubular form toward the vacuum port.

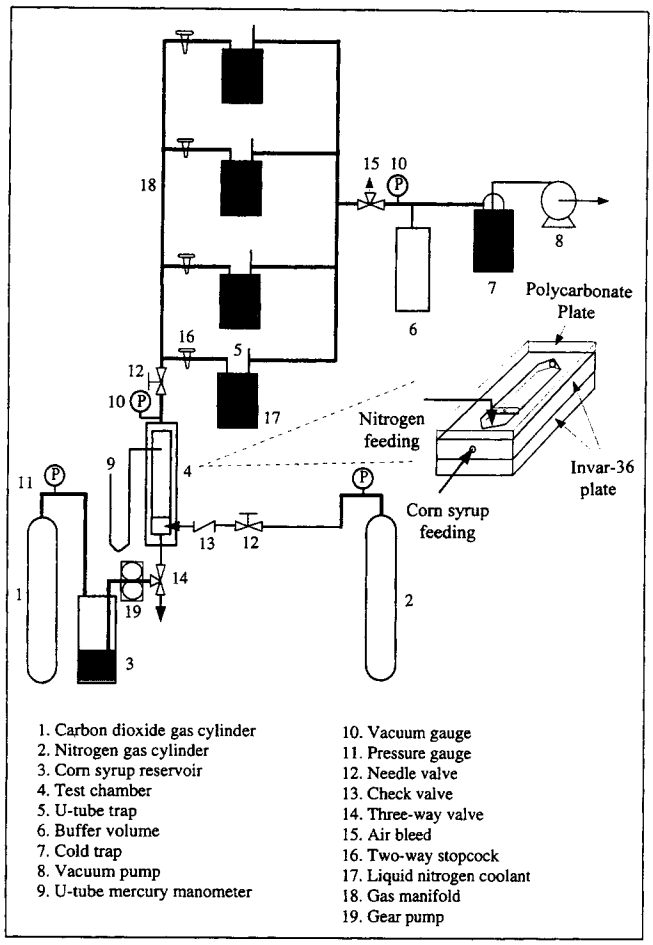

Figure 1. Process flow sheet for the corn syrup foaming experiment.

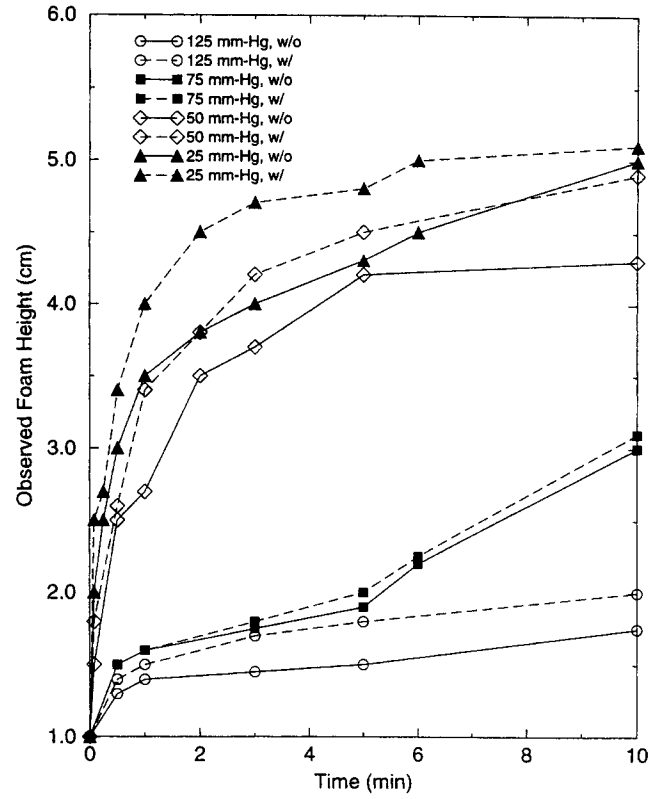

Figure 2. Observed foam height with time when the initial carbon dioxide concentration is 0.14 wt. %.

P_{go} = 60 psig (515 kPa).

After a certain amount of time, the foam structure collapsed at the foam surface and released volatiles.

At 50 mm Hg (7 kPa) vacuum, significant foam growth was observed. However, the foaming was not as vigorous as at 25 mm Hg (3 kPa) vacuum condition. Almost no foam rupture was seen near the foam free surface. The foam also grew roughly fives times by volume. At 75 mm Hg (10 kPa) vacuum condition, a moderate degree of bubble growth was observed. At 125 mm Hg (17 kPa) vacuum, no significant bubble growth was observed at the early stage. Later on, the color of the corn syrup became cloudy white. We believed that many small bubbles were nucleated in the corn syrup and grew. At 200 mm Hg (27 kPa) vacuum, not many bubbles were observed and they did not grow appreciably. At 380 mm Hg (51 kPa) vacuum, the corn syrup was essentially bubble free. Mass transfer of carbon dioxide was achieved by simply diffusing through the corn syrup surface. The observations are shown in Figure 3.

Experimental results using carbon dioxide with 30 psig (308 kPa) initial pressure (0.085 wt. % initial carbon dioxide concentration) showed that similar bubble dynamics with less foam intensity were observed at various vacuum conditions. The developing foam height with time, at various vacuum conditions, is shown in Figure 4. From Figures 2 and 4, we determined that the initial volatile concentration has little effect on the final foam volume. The final foam reached a constant volume in the range of 4.5 to 5 times the initial volume when the vacuum pressure is low enough to cause foaming

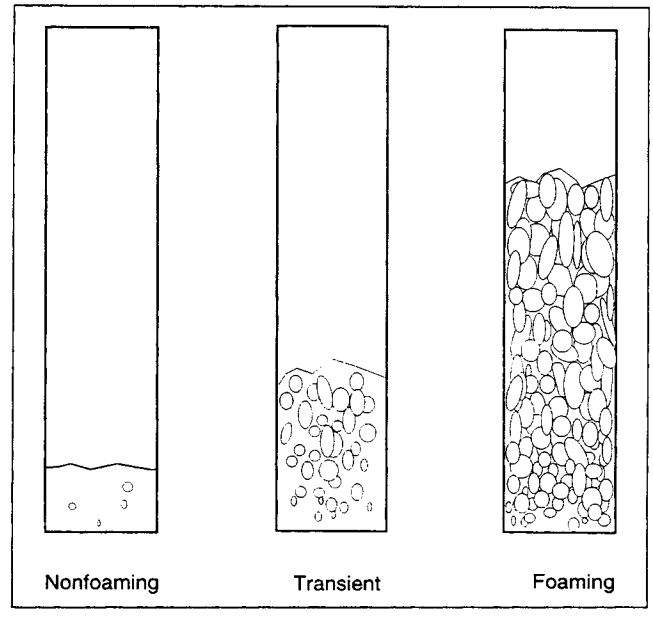

Figure 3. Experimental observations.

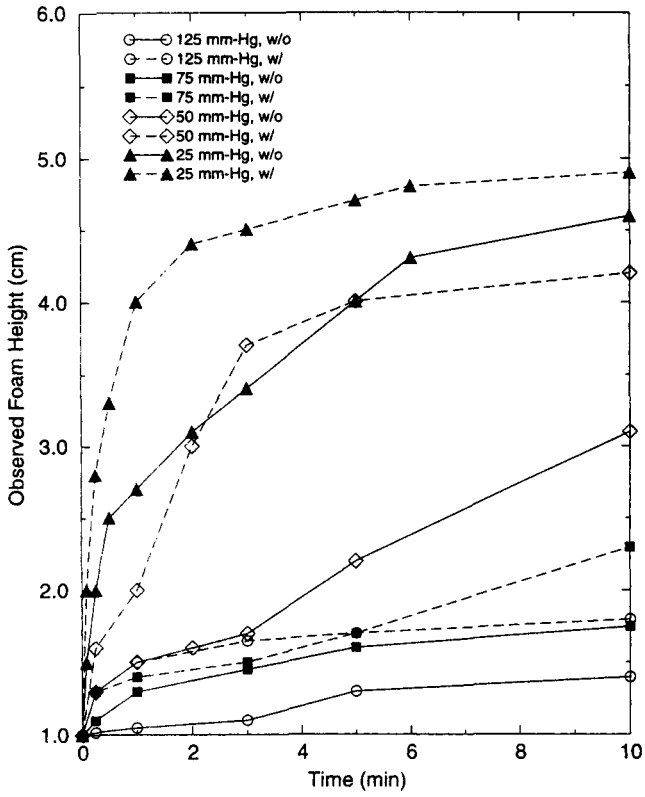

Figure 4. Observed foam height with time when the initial carbon dioxide concentration is 0.085 wt. %.

P_{go} = 30 psig (308 kPa).

and surface rupture [25 mm Hg (3 kPa)]. More research needs to be done to determine whether this constant foam volume is universal or is specific to this polymer/volatile system. Other factors may also affect the foam growth such as viscosity, elasticity, surface tension and melt strength (normal stress on the bubble surface due to growth) of the polymer.

Stripping Agent Effects. Nitrogent (0.1 wt. %) was used to determine the effect of a stripping agent on devolatilization performance. Nitrogen was initially dispersed in the corn syrup pool as bubbles (about 0.2 volume fraction). Experimental results showed that nitrogen increased foam growth rate. A shown in Figures 2 and 4, nitrogen reduced the time for the system to reach the same foam volume at the same vacuum condition. The foam also reached about 4.5 to 5 times the initial volume when foaming and surface rupture occurred [25 mm Hg (3 kPa)]. Therefore, when the desired condition of foaming and surface rupture was reached, the stripping agent had little effect on the final foam volume. The major role of a stripping agent was to enhance the foam growth rate. At higher vacuum pressures [380 and 200 mm Hg (51 and 27 kPa)], however, these nitrogen bubbles did not result in a significant increase in foam growth rate.

The model fluid-corn syrup experiments helped us understand the effect of vacuum level and stripping agent on devolatilization. For efficient devolatilization (that is, the constant foam volume was reached), the vacuum level must be high enough to create foam growth and rupture. In this case, we determined that 25, sometimes 50 mm Hg, vacuum pressure was sufficient. The role of stripping agents is to enhance foam growth rate and shorten the time needed for efficient devolatilization.

It is worthwhile to look into the effect of the number and size of stripping agent bubbles on foaming. Due to constraints of this current experimental apparatus, it is difficult to control the initial number and size of nitrogen bubbles in the corn syrup pool. Another method to quantitatively examine the effect of the initial number and size of nitrogen bubbles on foaming is reported in Yang et al. (1997).

Low-density polyethylene

The objective of the foaming experiments using low-density polyethylene (LDPE) is to determine the effect of dissolved stripping agent content (nitrogen) on devolatilization. A sorption experiment was conducted to measure the diffusivity and solubility of nitrogen in LDPE at 220°C and 400 psig (2.86 MPa) (Anolick and Chu, 1994). The nitrogen diffusivity and solubility in LDPE were found to be 5.2×10^{-5} cm^2/s and 1.9 wt. % (or 6.7×10^{-4} g/g atm) at 220°C and 400 psig (2.86 MPa), respectively.

The foaming experiment was performed in a test tube which was placed in an enclosed barricade with a heated cell. This enclosed barricade was equipped with a glass window for viewing. The development of the foam was recorded by time lapse photography. LDPE pellets of known weight were placed in the test tube and the system was operated at 200°C and under 400 psig (2.86 MPa) nitrogen. The system was exposed to nitrogen at the condition for different times (10, 20, 45, 60, 90 and 120 min). The initial nitrogen content can be determined by the diffusivity and solubility of nitrogen in LDPE. Then the nitrogen was released and vacuum (2 to 3.5 psia) was applied to the system.

Polymer melt was observed to foam instantaneously after the vacuum was applied. Foam breakup at the free surface was observed. Figure 5 shows the observed maximum foam volume change at various nitrogen holding times or concentrations. The foam volume change increases initially with holding time (or nitrogen concentration in LDPE). However, the maximum foam volume change reached a maximum (about 5 times the original volume) after holding time was above 45 min (or nitrogen content above 0.76 wt. %). The results suggest that the characteristic limiting maximum foam volume change for LDPE is about 5 times the initial polymer volume. There is an optimum amount of stripping agent needed to create a maximum foam volume for efficient devolatilization in LDPE.

From the batch foaming experiments with corn syrup and LDPE, we found that there is a limiting maximum foam volume expansion for a polymer when foaming and surface breakup occur in devolatilization. We recognize the limitations of using corn syrup as a model polymer in the batch foaming experiments such as a lack of elasticity and low viscosity. Nevertheless, both foaming experiments with corn syrup and LDPE provide some common observations and basis for our model development and more experiments. The visualization experimental method with corn syrup at room temperature allows one to observe the process in a slower manner for better understanding toward the devolatilization

mechanisms. One should not take the experimental results based on the model polymer and apply to real polymer systems without recognizing the differences in physical properties and process conditions. The validity of using model polymer at room temperature and synthetic polymer at high temperature for comparison of the devolatilization process will be discussed later.

The characteristic foam volume change for a polymer is an important parameter in designing proper screw arrangements and operating conditions for optimum devolatilization results. For example, to optimize LDPE devolatilization in an extruder, one may design the screw arrangements and operating conditions for a 20% degree of channel fill in the vacuum section as the first trial run without blindly conducting a series of extruder experiments. In this respect, this simple and quick information provides a cost-effective way of saving time for process development and saving capital expenditure for numerous actual extruder trial runs. As long as the characteristic foam volume expansion for a polymer is known by the batch foaming experiment, one can easily use this information to develop and optimize the devolatilization process for different polymers and in different sizes of the extruder machine.

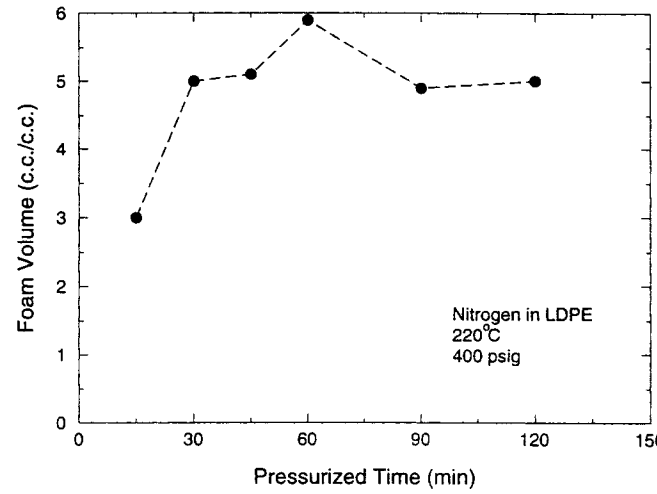

Figure 5. Observed foam volume growth vs. nitrogen holding times in foaming experiment with LDPE.

Model Development

As discussed above, a stripping agent does not have sufficient time to dissolve in the polymer due to its short residence time in the stripper injection section and its low diffusion coefficient in the polymer. A predominant fraction of the stripping agent should stay in the gas phase either dispersing in the polymer as bubbles or sweeping through over the polymer surface. We assume that the stripping agent disperses in the polymer as bubbles. Then we would like to develop a mathematical model to examine the effect of stripper bubbles on foaming dynamics and devolatilization performance.

Bimodal model for foam growth

A bimodal model for foam growth was first developed based on the cell model for bubble growth (Denson, 1983; Amon and Denson, 1984; Powell, 1987). Referring to Figure 6, the bimodal model for foam growth involves two bubble populations in the polymer: volatile bubbles and stripper bubbles. Each population has a characteristic number and size of bubbles. The dissolved volatile component can diffuse into both the volatile bubbles and the stripper bubbles during devolatilization. Initially, the stripper bubbles only contain the stripper gas molecules. As a vacuum is applied to the system, stripper bubbles grow as a result of volume expansion and diffusion of the volatile from the polymer. Each stripper bubble is also regarded as an isolated system such that no mass transfer of the stripper molecules outside the polymer film occurs during growth.

The governing equations along with their initial and boundary conditions for the growth dynamics of a single cell are listed in the Appendix. Refer to the work of Yang (1995) for a detailed derivation. Based on the model concepts discussed and the dynamics of a single cell growth, the following assumptions summarize the approach to formulate the bimodal model for foam growth.

(1) The stripping agent is dispersed in the polymer as bubbles, and volatile bubble nucleation is instantaneous.

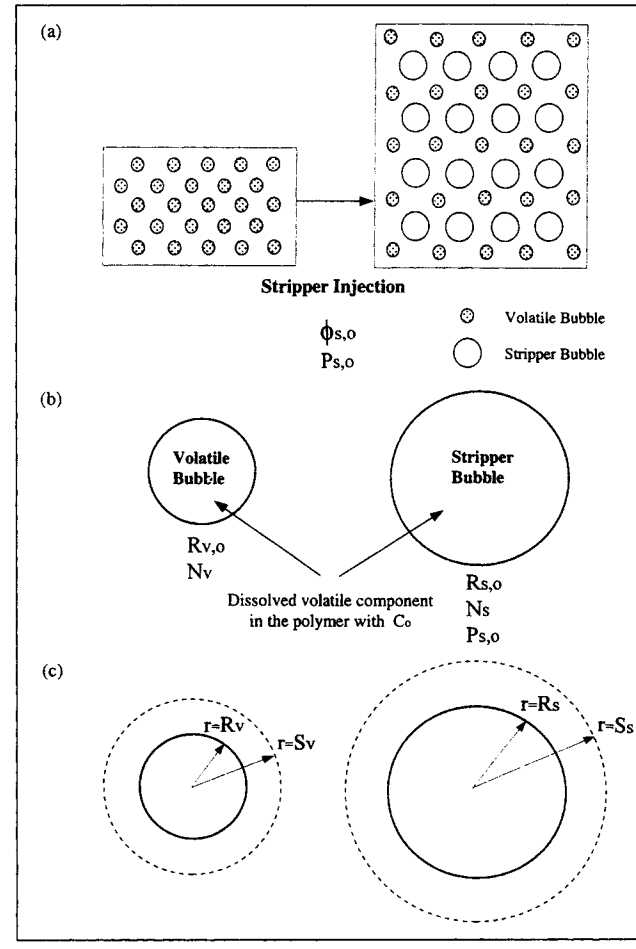

Figure 6. Bimodal model for foam growth.

(2) Initially, the partial vapor pressure of the volatile component in the stripper bubbles is assumed to be zero.

(3) The contributions of the volatile bubbles and the stripper bubbles on devolatilization are additive.

(4) With the incorporation of the stripper bubbles in the polymer, the amount of polymer assigned to each cell is divided such that there is an equal polymer film thickness surrounding the volatile bubbles and the stripper bubbles at any time. In other words, the volatile bubbles and stripper bubbles are equally spaced in the polymer during the growth process (see Figure 6).

An important issue of the bimodal model in numerical simulation is to redistribute the polymer volume between the volatile and stripper bubbles such that all bubbles are equally spaced at any time iteration. Following the development of the cell model for bubble growth, the bubble volume and polymer volume in a cell at any time is related by

$$\frac{4}{3}\pi S_v^3 = \frac{4}{3}\pi R_v^3 + \frac{4}{3}\pi V_v \tag{1}$$

$$\frac{4}{3}\pi S_s^3 = \frac{4}{3}\pi R_s^3 + \frac{4}{3}\pi V_s \tag{2}$$

where V_v and V_s are the polymer volumes in the volatile bubbles and the stripper bubbles divided by $4\pi/3$, respectively. N_v and N_s are constant numbers of the volatile bubbles and the stripper bubbles, respectively. The conservation of the polymer volume is described as follows

$$1 = N_v\left(\frac{4}{3}\pi V_v\right) + N_s\left(\frac{4}{3}\pi V_s\right) \tag{3}$$

At each time iteration, V_v and V_s are redistributed such that the thickness (δ, m) of the polymer film is the same in the volatile and stripper bubbles. That is,

$$S_v - R_v = \delta = S_s - R_s \tag{4}$$

or

$$(R_v^3 + V_v)^{1/3} - R_v = \delta = (R_s^3 + V_s)^{1/3} - R_s \tag{5}$$

V_v and V_s are solved simultaneously and substituted into the governing equations for cell growth. The calculated bubble radii are the inputs for solving the polymer volumes in the next time iteration for the bubbles to grow. As with the cell model for bubble growth, the bimodal model for foam growth considers the diffusion of the volatile component into the volatile and stripper bubbles as "devolatilization." This may not be adequate in that the foam volume may be unrealistically large if all the volatile component diffuses into the bubbles.

Film model for mass transfer

From observations of the foaming experiment, there is a maximum foam volume for a polymer to grow and sustain in which foaming and surface breakup occur. The polymer becomes an open-cell structure with thin polymer films providing a free path for the volatile to escape. Beyond this point, devolatilization is achieved by diffusion of the volatile component from the polymer films to the contiguous gas phase.

The mass-transfer problem of sorption and desorption through a polymer has been investigated in the literature (Crank and Park, 1968). Based on a simple sorption and desorption kinetics, mass transfer of a volatile component through a polymer film can be considered as diffusion of the component through the surface of a plane sheet of constant thickness δ. Figure 7 shows the film model for mass transfer. The initial volatile concentration (g/g) in the polymer is uniform throughout the polymer at constant C_o. At time zero, the polymer film is suddenly exposed to a constant equilibrium concentration C_e at the interface. In our case, C_e is lower than C_o so that mass transfer is a desorption or devolatilization. Referring to Figure 7, the arrows show that the direction of mass transfer for devolatilization is from the polymer to the contiguous gas phase.

The governing equation for mass transfer and the corresponding initial and boundary conditions are shown below.

$$\frac{\partial C}{\partial t} = D\frac{\partial^2 C}{\partial x^2} \tag{6}$$

$$I.C.: t = 0, \text{ any } x;\ C = C_o \tag{7}$$

$$B.C.s: t > 0,\ x = \pm\frac{\delta}{2};\ C = C_e \tag{8}$$

where D is the diffusion coefficient (cm^2/s) of the volatile component in the polymer and δ is the polymer film thickness. This parabolic partial differential equation can be solved analytically to calculate the volatile concentration in the polymer as a function of distance and time. The average volatile concentration remaining in the polymer film with time (s) $C_f(t)$ is obtained by integrating the volatile concentration along the film thickness and is expressed as

$$\frac{C_f(t) - C_e}{C_o - C_e} = \frac{2}{\pi}\sum_{n=0}^{\infty}\frac{1}{\left(n+\frac{1}{2}\right)^2}\exp\left(-\left(n+\frac{1}{2}\right)^2\left(\frac{2\pi}{\delta}\right)^2 Dt\right) \tag{9}$$

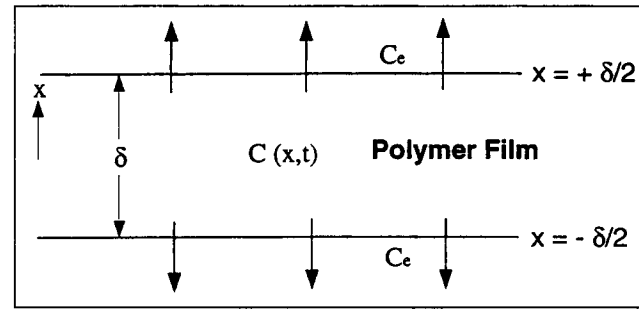

Figure 7. Film model for mass transfer.

Thermodynamic devolatilization efficiency TDE, %, is used to indicate the devolatilization performance and is defined as

$$\mathrm{TDE}(t)\% = \left(1 - \frac{C_f(t) - C_e}{C_o - C_e}\right) \times 100\% = \frac{C_o - C_f(t)}{C_o - C_e} \times 100\% \tag{10}$$

Basic Feature

Figure 8 shows the basic feature of our model for devolatilization by combining the bimodal model for foam growth with the film model for devolatilization. The mass-transfer mechanisms for devolatilization in both models are also shown in the plot.

Initially in Stage A, there are two bubble populations present in the polymer: (1) homogeneous nucleation of the volatile bubbles and (2) dispersion of the stripper bubbles. As the external pressure is reduced, the volatile bubbles and stripper bubbles grow in the polymer pool, as in Stage B. When the bubbles grow and foam to the point in which cells break on the free surface, Stage C is attained. Under this condition, the polymer looks like an open-cell web-like structure with thin polymer films providing a free path for volatile diffusion and escape. Beyond this point at Stage D, we model the devolatilization process as mass transfer through the thin polymer films. The basic feature of our model can be recognized in four stages in the following. The mathematical description of the model during foam development is also listed.

- Stage A: Volatile bubble nucleation and stripper bubble dispersion ($\phi_g = \phi_{v,o} + \phi_{s,o}$)
- Stage B: Bubble growth and foaming ($\phi_g = \phi_v + \phi_s$)
- Stage C: Foaming and surface breakup ($\phi_g = \phi_{\mathrm{crit}}$)
- Stage D: Foam breakup with thin polymer films in a web-like structure ($\phi_g > \phi_{\mathrm{crit}}$)

Thus, the first step of devolatilization is modeled by diffusion of the dissolved volatile component from the polymer to the volatile and stripper bubbles. As the foam volume reaches a critical condition, the film model for mass transfer is used to continue the computation. The second step of devolatilization is modeled by diffusion of the volatile component from polymer films to the gas phase and extracted by the vacuum.

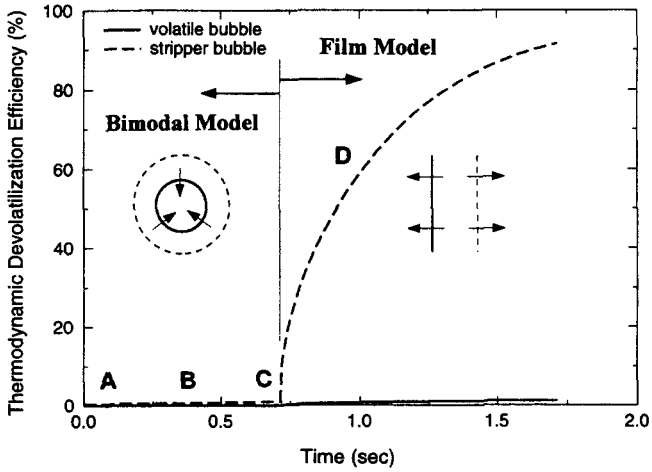

Figure 8. Bimodal model for foam growth and film model for mass transfer for devolatilization.

C_o = 1,825 ppm; $P_{s,o}$ = 0.79 MPa; N_s = 1,000 no./cm^3 liq.; P_{vac} = 25 mm Hg (3 kPa).

Table 1. Values of Three Levels for Five Factors in Factorial Experiment

Factor/Level	Low	Medium	High
$\phi_{s,o}$ (cm^3 gas/cm^3 liq.)	0.5	1.0	1.5
N_s (no./cm^3 liq.)	500	2,000	5,000
ϕ_{crit} (cm^3 gas/cm^3 liq.)	2.0	4.0	5.0
P_{vac} (mm Hg)	25	50	75
t (s)	3.0	5.0	7.0

Dynamics of Foam Devolatilization

This section demonstrates the dynamic behavior of foam devolatilization obtained by using the bimodal model for foam growth and the film model for devolatilization. Several important process variables and operating conditions are selected to examine their effects on the devolatilization performance.

A factorial experiment is designed to examine the effect of five important parameters on polymer devolatilization. The dependent variable (response) is the thermodynamic devolatilization. The dependent variable (response) is the thermodynamic devolatilization efficiency (TDE). The independent variables (factors) are the initial stripper volume fraction ($\phi_{s,o}$) (cm^3 gas/cm^3 liq.), the number of stripper bubbles (N_s) (no./cm^3 liq.), the critical gas volume fraction (ϕ_{crit}), vacuum pressure (P_{vac}), and time (t). Each factor is varied at three levels. The numerical values corresponding to each level of the factors are listed in Table 1. The physical properties of the devolatilization system are listed in Table 2. The number of volatile bubbles in this sample calculation is 5,000/cm^3 liq. We believe that the five factors and their levels in Table 2 in model demonstration are reasonable from our experimental observation and experience. Under high injection pressure, the initial stripper volume should be small. In the foaming experiments, the number of bubbles observed was on the order of 100 to 1,000/cm^3 liq. The same observation was made by Newman and Simon (1980) in their study of polystyrene/styrene devolatilization in a falling-strand type equipment. The critical volume expansion was 4 to 5 times for the polymers investigated in this work. It may be difficult to foam up some polymers due to their physical properties or poor design and conditions in the devolatilization zone. The average residence time for devolatilization in the extruder is fractions of a minute. One should note that the selection of these conditions is for a model demonstration and could be varied to examine the results.

Table 2. Physical Properties of Devolatilization System Used for Bimodal/Film Model in Factorial Experiment

Properties	Values
Diffusion coefficient	1.92×10^{-5} cm^2/s
Henry's law constant	3,567.28 atm
Polymer density	1.4 g/cm^3
Surface tension	40 dyne/cm
Polymer viscosity	56 Pa·s

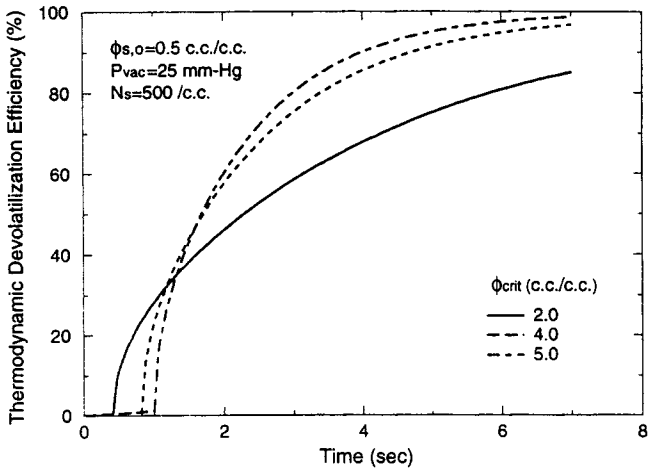

Figure 9. Dynamics of foam devolatilization: $\phi_{s,o} = 0.5$ cm^3 gas/cm^3 liq.; $N_s = 500$ no. cm^3/liq.; $P_{vac} = 25$ mm Hg (3 kPa).

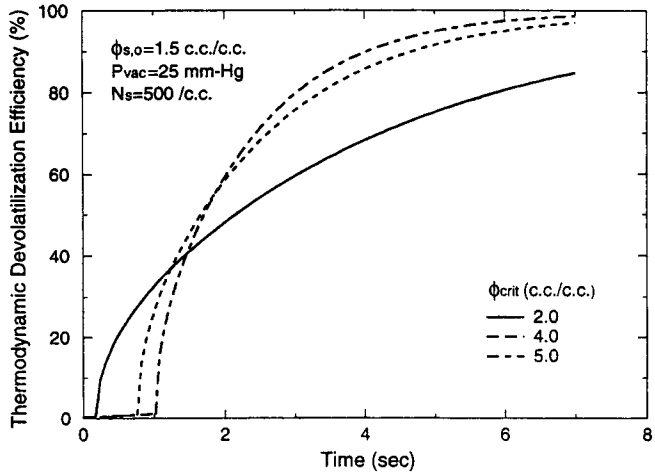

Figure 10. Dynamics of foam devolatilization: $\phi_{s,o} = 1.5$ cm^3 gas/cm^3 liq.; $N_s = 500$ no./cm^3 liq.; $P_{vac} = 25$ mm Hg (3 kPa).

For a full 3^5 factorial experimental design, there are 243 combination treatments. The numerical computation for all 243 cases has been performed using the bimodal model for foam growth combined with the film model for devolatilization according to the process conditions in each factor-level combination. Several characteristics of the foam dynamics for devolatilization are recognized and illustrated from the numerical experiment. Figure 9 shows the thermodynamic devolatilization efficiency vs. time when the initial stripper volume fraction is 0.5 cm^3 gas/cm^3 liq.; the number of stripper bubbles is 500 no./cm^3 liq.; and the vacuum pressure is 25 mmHg (3 kPa). The critical gas volume fractions are 2.0, 4.0 and 5.0 cm^3 gas/cm^3 liq. It is seen that as the critical gas volume fraction increases from 2.0 to 4.0 and 5.0 cm^3 gas/cm^3 liq., the critical time for making the transition from the bimodal model to the film model is delayed. However, by taking a little more time for the foam to grow and to make the polymer film surrounding the bubbles thinner, the subsequent rate of mass transfer increases, thereby reaching a higher devolatilization efficiency at a later time.

In other words, if we do not design a proper devolatilization section which allows for the desired foam volume change (such as 5 times the initial polymer volume), foaming is constrained and/or the foam breaks earlier than desired, resulting in a lower degree of devolatilization efficiency. Therefore, it is very important to design a devolatilization section which accommodates the unconstrained free foaming of the polymer. Foster and Lindt (1989) studied devolatilization in a 20-mm counterrotating tangential twin-screw extruder. They found that at a constant screw speed, the mass-transfer coefficient for devolatilization increased with increasing polymer throughout, but began to decrease after a critical throughput (or degree of fill) was reached. It suggested that the screw channel at a higher degree of fill did not provide sufficient free volume to accommodate the desired foam expansion. As a result, foam growth was constrained by the screw channel. A low effective mass-transfer coefficient for devolatilization was obtained.

Figure 10 shows the devolatilization results under the same conditions as in Figure 9 except that the initial stripper volume fraction is 1.5 cm^3 gas/cm^3 liq. Almost the same dynamic behavior of devolatilization process is observed as in Figure 9. The initial stripper volume fraction shows little effect on the devolatilization dynamics and the final devolatilization performance.

Figure 11 shows the devolatilization results at the same conditions as in Figure 9 except that the number of stripper bubbles is increased to 5,000 no./cm^3 liq. Similar devolatilization trends are observed as in Figure 9. An increase in the number of stripper bubbles, however, makes the transition from the bimodal model to the film model occur within a shorter period of time. That is, a greater number of stripper bubbles makes the polymer foam faster to the critical foam volume so that the film model for mass transfer takes over the devolatilization process. As a result, the thickness of the polymer film surrounding the bubbles is thinner than shown in Figure 9. Later, a thinner polymer film thickness facilitates a faster rate of mass transfer and reaches a higher

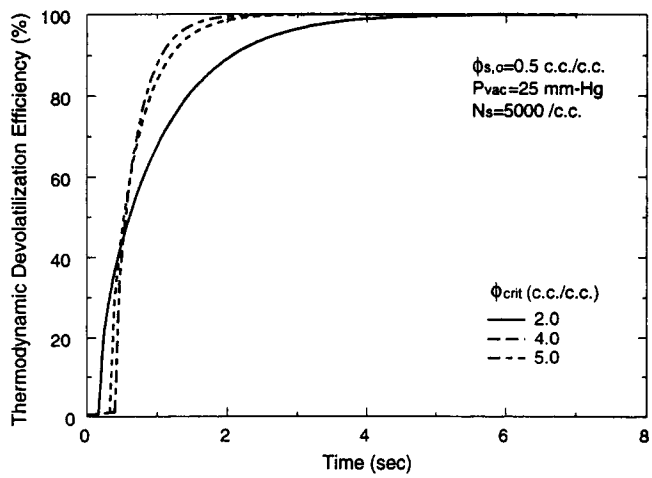

Figure 11. Dynamics of foam devolatilization: $\phi_{s,o} = 0.5$ cm^3/gas cm^3 liq.; $N_s = 5{,}000$ no./cm^3 liq.; $P_{vac} = 25$ mm Hg (3 kPa).

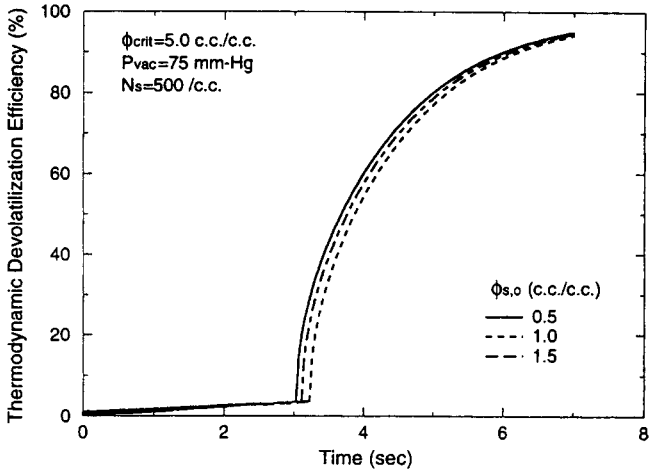

Figure 12. Dynamics of foam devolatilization: $\phi_{s,o} = 0.5$ cm^3 gas/cm^3 liq.; $N_s = 500$ no./cm^3 liq.; $\phi_{crit} = 5.0$ cm^3 gas/cm^3 liq; $P_{vac} = 75$ mm Hg (10 kPa).

devolatilization efficiency, as seen in Figure 11. Therefore, the number of stripper bubbles plays an important role in accelerating the foam growth rate and enhancing the devolatilization performance.

Figure 12 shows the devolatilization results under conditions in which the foam growth does not reach the desired foam volume expansion. The number of stripper bubbles is 500 no./cm^3 liq., the critical gas volume fraction is 5.0 cm^3 gas/cm^3 liq., and the vacuum pressure is 75 mm Hg (10 kPa). The foam growth does not reach the desired fivefold expansion by the 3-s residence time. The film model is not used to complete the devolatilization computation. Only the bimodal model completely covers the devolatilization process and shows poor devolatilization results under the process time (3 s) investigated. As shown in Figure 12, about 3% thermodynamic devolatilization efficiency is achieved at the 3-s process time when the initial stripper volume fraction is 0.5, 1.0 and 1.5 cm^3 gas/cm^3 liq. These are the only three conditions in the factorial experiment under which the film model for mass transfer is not used to complete the devolatilization process. Therefore, in this set of process conditions we should avoid operating the devolatilization process for less than a 3-s mean residence time in order to allow for the desired fivefold foam expansion and achieve a higher thermodynamic devolatilization efficiency.

As mentioned in the literature, the foam devolatilization process is mass-transfer-controlled and dominated by diffusion of volatile into the bubbles and to the contiguous vapor space. In the development of bimodal/film model for devolatilization, the characteristic time for mass transfer t_D is an appropriate time scale for foam devolatilization. (See Appendix: $t_D \sim 1/D$.) By comparing the diffusion coefficient of a low-molecular-weight volatile gas such as nitrogen in corn syrup at room temperature (on the order of 10^{-7} to 10^{-8} cm^2/s) with that in LDPE at high temperature (on the order of 10^{-5} to 10^{-6} cm^2/s) one can find that the difference in time scales for diffusion is about 10 to 100. The difference in the process time scales for foam devolatilization with corn syrup and LDPE is about on the same order of 10 to 100 (10 min vs. 10 s or fractions of a min). The dimensionless time scales for both systems are falling into the same order of magnitude. ($\tilde{t} = t/t_D \sim t \times D$). In this respect, the results of foaming experiments with a model polymer at room temperature are applicable to those with the synthetic polymer at high temperature.

One also should consider the operation of the devolatilization section as an integral part of the whole extruder process design and optimization. The various extruder stage operations in solid feeding and melting, dispersive and distributive mixing, compounding of additives and fillers, incorporation of processing aids, devolatilization and deaeration, pressurization and pumping should be considered together as an integrated process development and optimization. The issue in this study is to design a devolatilization section that has sufficient mean residence time and free volume in the screw channel to allow for the desired full foam volume expansion and to approach the thermodynamic equilibrium limits in devolatilization, while optimized with respect to the production rate requirement.

One of the areas of devolatilization that we did not research was the area of bubble nucleation mechanisms. The problem with any cell model for devolatilization is that, for a given volume fraction, the initial number and size distribution of the bubbles is not known. The first question concerns what is the initial number and size of the stripper bubbles. The second issue is about what effect the stripper gas has on the homogeneous nucleation of the volatile. Each of these questions could warrant a major research effort in its own right. We found little has been done to address the second issue in terms of model prediction, because the initial size of the volatile bubbles and the chemical potential driving force is much less than that for the stripper bubbles. In other words, most of the volatile removal and the rapid pool growth occurs due to the existence of the unidissolved stripper bubbles. In addition, the initial number and size of volatile and stripper bubbles play a secondary role into the model prediction. The key parameter is the volume at which it is assumed that the foam breaks. That assumption determines the film thickness which is the ultimate physical parameter determining the model prediction for devolatilization rate and ultimate thermodynamic devolatilization efficiency.

In the parametric study of dynamics of foam devolatilization, we found that the rate of foam growth for the stripper bubbles is significantly faster than that for the volatile bubbles. We determine that stripper bubbles contribute to over 85% of the total devolatilization efficiency. Therefore, the number of volatile bubbles is not important.

The biomodal/film model developed in this work and applied to an extruder process does not include shear rate effects. Shear rate affects the devolatilization at many levels including enhanced bubble nucleation due to mechanical stress and stretching (Tukachinsky et al., 1994) and cavitation (Biesenberger and Lee, 1987a; Lee and Biesenberger, 1989), bubble elongation and rupture (Biesenberger and Lee, 1987b), and foam compression and collapse (Biesenberger and Lee, 1987a,b; Lee and Biesenberger, 1989; Tukachinsky et al., 1994). Each of these phenomena should be considered in the devolatilization process as they affect all stages of foaming, namely, bubble nucleation, growth, coalescence, and breakage. Yet, the model presented in this work has shown

improvements and is better than either the pool model or the cell model. The reason why the shear rate is not a primary parameter lies in the characteristic times for different parts of the process. In an extruder, our experiments and calculations have shown that when there is rapid foam volume growth, the polymer pool can grow to 4 to 5 times its original volume on the order of 0.5 s. The shear rate manifests on the process by deforming the polymer pool. Therefore, a viable measure of the characteristic time for shear rate is the time it takes for the pool to rotate once in the screw channel. If the screw speed is 120 rpm, then the screw rotates once every 0.5 s. One can compute that the pool rotates once for every one-and-half screw rotations. Therefore, the characteristic time for shear rate is 0.75 s. Physically, this implies that as the polymer enters into the devolatilization region, the polymer undergoes a rapid growth due to the supersaturation in chemical potential. It can complete the pool volume growth before the major effects of the shear rate can come into play. It would seem that at that point the three effects described above would still come into play, and it would have to be determined whether shear rate enhances or suppresses the devolatilization process. Since the most important variable for the computation of thermodynamic devolatilization efficiency in this model is the critical foam volume expansion, shear rate seems to only play a secondary role to that parameter.

Conclusions

Removal of volatile components from a polymer melt by the decrease of pressure sometimes results in bubbling or foaming, in which case the devolatilization process is more rapid than when the devolatilization is one of molecular diffusion alone. In this study, corn syrup and LDPE were used to investigate the effects of volatile content, vacuum pressure and stripping agent in the devolatilization process. Observations from the foaming experiments showed that there is a threshold of vacuum conditions beyond which foaming occurs. Beyond that threshold, the foam can grow to a maximum volume where surface rupture occurs. The conditions of expanding gases and final pressures that produce these maximum foam volumes also give the higher devolatilization efficiency. Vacuum pressures as low as 25 mm Hg (3 kPa) were needed, although 50 mmHg (7 kPa) was sometimes sufficient. Increased stripping agent or volatile content had little effect on the final foam volume. Although the stripping agent had little effect on the final foam volume, it did enhance the foam growth, increase devolatilization efficiency, and decrease the volatile fraction to about 1/4 to 1/2 of the amount without nitrogen.

We conclude that the devolatilization process is most efficient where there is sufficient evaporating gases to foam the melt and produce expansion of the maximum foam volume (for these fluids, the maximum is a 4 to 5 fold expansion). Above this maximum, the foam is open cell and evaporating gases escape easily, so that the evaporation of volatiles is not restricted by diffusion. Stripping agents help devolatilization in three ways: they allow the maximum foam volume to be reached in less severe conditions of vacuum, accelerate the foam growth, and decrease the partial pressure of the evaporating component in the growth bubbles. From the free-volume theory for prediction of diffusion coefficient and from the consideration of the low diffusion coefficients of stripping agents in the polymer, it is suggested that there is not sufficient time for the stripping agents to dissolve in the polymer due to the short residence time in the extruder (typically 5 to 10 s). Aligned with this finding, we assume that the stripping agent only disperses in the polymer as bubbles.

A mathematical model is developed to examine the effect of stripper bubbles in polymer devolatilization. Basic features of our model are illustrated. Our model takes into account the observation of a limiting foam volume for a specific polymer to grow and sustain. Based on the cell model for bubble growth, a bimodal model for foam growth is developed to describe the initial growth of the volatile and stripper bubbles. When the polymer expands to a critical foam volume where foam breakup occurs, the film model for devolatilization is used to model the second step of devolatilization.

Several dynamic behaviors of foam devolatilization in our model are demonstrated based on a numerical experiment. The results of this factorial experimental design suggest several important process design and operation considerations in extruder devolatilization. The devolatilization section should be designed and operated in conditions such that the screw channel provides sufficient free volume to accommodate the desired polymer pool expansion. Otherwise, foaming is constrained and/or foam breaks earlier than desired, resulting in a low degree of thermodynamic devolatilization efficiency. In addition, one needs to consider the issue of residence time in the devolatilization section. We have shown that if the polymer does not have sufficient residence time to fully expand to the desired volume, the devolatilization efficiency would be low. The process development and optimization in the devolatilization section should be considered as an integral part of the whole extruder design and operation.

Acknowledgments

The authors would like to gratefully acknowledge the financial support from DuPont Central Research and Development, Wilmington, DE.

Notation

H_w = Henry's law constant, atm
M = molecular weight, g/mol
P = pressure, Pa
P_{vac} = vacuum pressure, mmHg
R = bubble radius, cm
R_g = gas constant, atm·cm^3/mol·K
S = cell radius, cm
T = temperature, °C
V_L = polymer volume assigned to each cell divided by $4\pi/3$, cm^3
w = weight fraction, g/g
x = distance, cm
η = viscosity, Pa·s
ρ = density, g/cm^3
σ = interfacial tension, dyne/cm
τ = stress, dyne/cm^2

Subscripts

f = final
g = gas
L = liquid

Literature Cited

Albalak, R., Z. Tadmor, and Y. Talmon, "Scanning Electron Microscopy Studies of Polymer Melt Devolatilization," *AIChE J.*, **33**, 808 (1987).

Albalak, R. J., *Polymer Devolatilization*, Marcel Dekker, New York (1996).

Albalak, R. J., Z. Tadmor, and Y. Talmon, "Polymer Melt Devolatilization Mechanisms," *AIChE J.*, **36**, 1313 (1990).

Amon, M., and C. D. Denson, "A Study of the Dynamics of Foam Growth: Analysis of the Growth of Closely Spaced Spherical Bubbles," *Poly. Eng. Sci.*, **24**, 1026 (1984).

Anolick, C., and J.-N. Chu, *Devolatilization Fundamentals—Nitrogen Solubility and Foam Kinetics*, DuPont, Wilmington, DE (1994).

Arefmanesh, A., and S. G. Advani, "Diffusion-Induced Growth of a Gas Bubble in a Viscoelastic Fluid," *Rheol. Acta*, **30**, 274 (1991).

Barth, U., G. Scheel, and M. Pahl, "The Multi-Screw Extruder 'MSE' for Nylon 6 Devolatilization and Post Condensations with PET," *SPE ANTEC*, p. 250 (1995).

Biesenberger, J. A., *Devolatilization of Polymers*, Hansen, New York (1983).

Biesenberger, J. A., and G. Kessidis, "Devolatilization of Polymer Melts in Single-Screw Extruders," *Poly. Eng. Sci.*, **22**, 832 (1982).

Biesenberger, J. A., and S.-T. Lee, "A Fundamental Study of Polymer Melt Devolatilization: I. Some Experiments on Foam-Enhanced Devolatilization," *Poly. Eng. Sci.*, **26**, 982 (1986a).

Biesenberger, J. A., and S.-T. Lee, "A Fundamental Study of Polymer Melt Devolatilization: II. A Theory for Foam-Enhanced Devolatilization," *SPE ANTEC*, p. 846 (1986b).

Biesenberger, J. A., and S.-T. Lee, "A Fundamental Study of Polymer Melt Devolatilization: III. More Experiments on Foam-Enhanced Devolatilization," *Poly. Eng. Sci.*, **27**, 510 (1987a).

Biesenberger, J. A., and S.-T. Lee, "A Fundamental Study of Polymer Melt Devolatilization: IV. Some Theories and Models for Foam-Enhanced Devolatilization," *SPE ANTEC*, p. 81 (1987b).

Biesenberger, J. A., and D. H. Sebastian, *Principles of Polymerization Engineering*, Wiley, New York (1983).

Blander, M., and J. L. Katz, "Bubble Nucleation in Liquids," *AIChE J.*, **21**, 833 (1975).

Collins, G. P., C. D. Denson, and G. Astarita, "Determination of Mass Transfer Coefficients for Bubble-Free Devolatilization of Polymeric Solutions in Twin-Screw Extruders," *AIChE J.*, **31**, 1288 (1985).

Coughlin, R. W., and G. P. Canevari, "Drying Polymers During Screw Extrusion," *AIChE J.*, **15**, 560 (1969).

Crank, J., and G. S. Park, *Diffusion in Polymers*, Academic Press, New York (1968).

Denson, C. D., "Stripping Operations in Polymer Processing," *Adv. in Chem. Eng.*, **12**, 61 (1983).

Foster, R. W., and J. T. Lindt, "Bubble Growth Controlled Devolatilization in Twin-Screw Extruders," *Poly. Eng. Sci.*, **29**, 178 (1989).

Foster, R. W., and J. T. Lindt, "Twin Screw Extrusion Devolatilization: From Foam to Bubble Free Mass Transfer," *Poly. Eng. Sci.*, **30**, 621 (1990).

Geol, S. K., and E. J. Beckman, "Nucleation and Growth in Microcellular Materials: Supercritical Carbon Dioxide as Foaming Agent," *AIChE J.*, **41**, 357 (1995).

Latinen, G. A., "Devolatilization of Viscous Polymer Systems," *Adv. Chem. Ser.*, **34**, 235 (1962).

Lee, S.-T., and J. A. Biesenberger, "A Fundamental Study of Polymer Melt Devolatilization. IV: Some Theories and Models for Foam-Enhanced Devolatilization," *Poly. Eng. Sci.*, **29**, 782 (1989).

Mack, M. H., and A. Pfeiffer, "Effect of Stripping Agents for the Devolatilizing of Highly Viscous Polymer Melts," *SPE ANTEC*, p. 1060 (1993).

Newman, R. E., and R. H. M. Simon, "A Mathematical Model of Devolatilization Promoted by Bubble Formation," *AIChE Meeting*, Chicago (1980).

Powell, K. G., "The Thinning and Growth of Gas Bubbles on Viscous Liquid/Gas Interfaces," PhD Thesis, Univ. of Delaware, Newark (1987).

Ramesh, N. S., D. H. Rasmussen, and G. A. Campbell, "Numerical and Experimental Studies of Bubble Growth During the Microcellular Foaming Process," *Poly. Eng. Sci.*, **31**, 1657 (1991).

Ravindranath, K., and R. A. Mashelkar, "Analysis of the Role of Stripping Agents in Polymer Devolatilization," *Chem. Eng. Sci.*, **43**, 429 (1988).

Roberts, G. W., "A Surface Renewal Model for the Drying of Polymers During Screw Extrusion," *AIChE J.*, **16**, 878 (1970).

Secor, R. M., "A Mass Transfer Model for a Twin-Screw Extruder," *Poly. Eng. Sci.*, **26**, 647 (1986).

Tukachinsky, A., Z. Tadmor, and Y. Talmon, "Ultrasound-Enhanced Devolatilization of Polymer Melt," *AIChE J.*, **39**, 359 (1993).

Tukachinsky, A., Y. Talmon, and Z. Tadmor, "Foam-Enhanced Devolatilization of Polystyrene Melt in a Vented Extruder," *AIChE J.*, **40**, 670 (1994).

Upadhyay, R. K., "Study of Bubble Growth in Foam Injection Molding," *Adv. in Poly. Technol.*, **5**, 55 (1984).

Vrentas, J. S., and J. L. Duda, "Diffusion of Small Molecules in Amorphous Polymers," *Macromol.*, **9**, 785 (1976).

Vrentas, J. S., and J. L. Duda, "Diffusion in Polymer-Solvent Systems: I. Reexamination of the Free-Volume Theory," *J. Poly. Sci.: Part B: Poly. Phys.*, **15**, 403 (1977a).

Vrentas, J. S., and J. L. Duda, "Diffusion in Polymer-Solvent Systems: II. A Predictive Theory for the Dependence of Diffusion Coefficient on Temperature, Concentration, and Molecular Weight," *J. Poly. Sci.: Part B: Poly. Phys.*, **15**, 417 (1977b).

Vrentas, J. S., J. L. Duda, and H.-C. Ling, "Enhancement of Impurities Removal from Polymer Films," *J. Appl. Poly. Sci.*, **30**, 4499 (1985).

Werner, H., *Devolatilisation of Plastics*, Verein Deutscher Ingenieure VDI-GmbH, Dusseldorf, Germany (1980).

Yang, C.-T., "A Study of Trace Devolatilization of Polymers," PhD Thesis, Univ. of Maryland at College Park (1995).

Yang, C.-T., D. I. Bigio, and T. G. Smith, "Prediction of Diffusion Coefficients in Polymer-Solvent Systems Using Free-Volume Theory," *Chem. Eng. Sci.*, (in press, 1996).

Yang, C.-T., T. G. Smith, D. I. Bigio, and C. Anolick, "A Mathematical Model for Polymer Devolatilization," *SPE ANTEC Tech. Papers*, p. 350, Indianapolis (1996a).

Yang, C.-T., T. G. Smith, D. I. Bigio, and C. Anolick, "Polymer Trace Devolatilization: Foam Experiments and Modeling," Paper 213b, AIChE Meeting, Chicago (1996b).

Yang, C-T., T. G. Smith, D. I. Bigio, and C. Anolick, "Polymer Trace Devolatilization: II. Case Study and Experimental Verification," *AIChE J.*, **43**(7), 1874 (July, 1997).

Yoo, H. J., and C. D. Han, "Development of a Mathematical Model of Foam Devolatilization," *Poly. Process Eng.*, **2**, 129 (1984).

Zielinski, J. M., and J. L. Duda, "Predicting Polymer/Solvent Diffusion Coefficients Using Free-Volume Theory," *AIChE J.*, **38**, 405 (1992).

Appendix: Analysis of Growth Dynamics of Single Cell

The growth dynamics of a single spherical bubble in a finite pool of a Newtonian fluid under isothermal conditions is summarized. The analysis is similar to the work of Amon and Denson (1984) and Powell (1987), but the scaling factor for the bubble radius is based on the initial bubble radius (Upadhyay, 1984; Arefmanesh and Advani, 1991; Ramesh et al., 1991; Geol and Beckman, 1995). The cell model assumes a constant bubble population in the fluid. Each cell consists of a spherical bubble and a finite liquid shell surrounding it. The spherical bubble only grows in the radial direction within the liquid shell.

The dimensionless variables are defined as follows

$$\tilde{y} = \frac{y}{S_o^3 - R_o^3} \tag{A1}$$

$$\tilde{t} = \frac{t}{R_o^2/D} \tag{A2}$$

$$\tilde{R} = \frac{R}{R_o} \tag{A3}$$

$$\tilde{P}_g = \frac{P_g}{P_{go}} \tag{A4}$$

$$\tilde{V}_L = \frac{V_L}{S_o^3 - R_o^3} \tag{A5}$$

$$\tilde{C} = \frac{C}{C_o} \tag{A6}$$

The governing equations in dimensionless form with their initial and boundary conditions are expressed in the following:

$$\tilde{P}_g - 2\frac{\Pi_\sigma}{\tilde{R}} - \tilde{P}_f - 4\frac{t_\eta}{t_D}\left(\frac{\tilde{V}_L}{\tilde{V}_L + \frac{\tilde{R}^3}{\Pi_\upsilon}}\right)\frac{d\tilde{R}}{d\tilde{t}} = 0 \tag{A7}$$

$$\frac{d}{d\tilde{t}}\left(\tilde{P}_g\tilde{R}^3\right) = 9\frac{\Pi_\rho}{\Pi_\upsilon^{1/3}}\tilde{R}^2\left(\tilde{y} + \frac{\tilde{R}^3}{\Pi_\upsilon}\right)^{2/3}\left.\frac{\partial\tilde{C}}{\partial\tilde{y}}\right|_{\tilde{y}=0} \tag{A8}$$

$$\frac{\partial\tilde{C}}{\partial\tilde{t}} = 9\frac{1}{\Pi_\upsilon^{2/3}}\frac{\partial}{\partial\tilde{y}}\left[\left(\tilde{y} + \frac{\tilde{R}^3}{\Pi_\upsilon}\right)^{4/3}\frac{\partial\tilde{C}}{\partial\tilde{y}}\right] \tag{A9}$$

$$\tilde{C}_{\text{avg}} = 1 - \frac{1}{\Pi_\upsilon\Pi_\rho}\left(\tilde{P}_g\tilde{R}^3 - 1\right) \tag{A10}$$

$$\tilde{R}(\tilde{t}=0) = 1 \tag{A11}$$

$$\tilde{P}_g(\tilde{t}=0) = 1 \tag{A12}$$

$$\tilde{C}(\tilde{y}=0,\tilde{t}) = \tilde{P}_g \tag{A13}$$

$$\tilde{C}(\tilde{y},\tilde{t}=0) = 0 \tag{A14}$$

$$\frac{\partial\tilde{C}}{\partial\tilde{y}}(\tilde{y}=1,\tilde{t}) = 0 \tag{A15}$$

Several dimensionless parameters arise on nondimensionalization of the governing equations along with their initial and boundary conditions

$$t_\eta = \frac{\eta}{P_{go}} \tag{A16}$$

$$t_D = \frac{R_o^2}{D} \tag{A17}$$

$$\Pi_\sigma = \frac{\sigma}{P_{go}R_o} \tag{A18}$$

$$\Pi_\upsilon = (S_o/R_o)^3 - 1 \tag{A19}$$

$$\Pi_\rho = \rho_L/H_w(R_gT/M) \tag{A20}$$

t_η is the characteristic time for momentum transfer (s), and t_D is the characteristic time for mass transfer by diffusion (s), respectively. Π_σ is the dimensionless surface tension $(\sigma/P_{go}R_o)$. Π_υ expresses the ratio of the initial volume of the liquid relative to the volume occupied by the bubble $[(S_o/R_o)^3 - 1]$. Π_ρ is the ratio of the liquid density to the density of the gas $[(\rho_L/H_w(R_gT/M)]$. The system of governing equations is nonlinear and highly coupled. A combination of the fourth-order Runge-Kutta and iterative finite difference scheme is used to solve them.

Manuscript received Apr. 22, 1996, and revision received Mar. 3, 1997.